

# Erosional and depositional characteristics of regional overwash deposits caused by multiple hurricanes

PING WANG\* and MARK H. HORWITZ†

\*Department of Geology, University of South Florida, 4202 E. Fowler Ave., Tampa, FL 33620, USA  
(E-mail: [pwang@cas.usf.edu](mailto:pwang@cas.usf.edu))

†BCI Engineers and Scientists, Inc., Lakeland, FL 33803, USA

## ABSTRACT

Regional-scale washover deposits along the Florida Gulf and Atlantic coasts induced by multiple hurricanes in 2004 and 2005 were studied through coring, trenching, ground-penetrating radar imaging, aerial photography, and prestorm and poststorm beach-profile surveys. Erosional and depositional characteristics in different barrier-island sub-environments, including dune field, interior wetland and back-barrier bay were examined. Over the eroded dune fields, the washover deposits are characterized by an extensive horizontal basal erosional surface truncating the old dune deposits and horizontal to slightly landward-dipping stratification. Over the marshes in the barrier-island interior, the washover deposits are characterized by steep tabular bedding, with no erosion at the bottom. Overwash into the back-barrier bay produced the thickest deposits characterized by steep, prograding sigmoidal bedding. No significant erosional feature was observed at the bottom. Washover deposits within the dense interior mangrove swamp demonstrate both normal and reversed graded bedding. The washover deposits caused by hurricanes Frances (2004) and Jeanne (2004) along the southern Florida Atlantic coast barrier islands are substantially different from those along the northern Florida barrier islands caused by Ivan (2004) and Dennis (2005) in terms of regional extension, erosional features and sedimentary structures. These differences are controlled by different overall barrier-island morphology, vegetation type and density, and sediment properties. The homogeneity of sediment along the northern Florida coast makes distinguishing between washover deposits from Ivan and Dennis difficult. In contrast, along the Atlantic coast barrier islands, the two overwash events, as demonstrated by two phases of graded bedding of the bimodal sediments, are easily distinguishable.

**Keywords** Barrier island, coastal erosion, Florida, ground-penetrating radar, hurricanes, overwash, storms, washover deposits.

## INTRODUCTION

One of the major morphologic impacts on beaches of powerful storms is overwash and the resulting washover deposits. Along relatively low-lying barrier islands, such as those in the northern Gulf of Mexico, regional-scale overwash often results from significant storm events (Stone *et al.*, 2005). In addition to wind transport, overwash provides a major mechanism for sediment redistribution above the high-tide line. Overwash

events are episodic and are characterized by rapid and dramatic sediment movement driven by extremely high energy. Understanding the erosional and depositional processes associated with regional overwash events is therefore crucial to understanding barrier-island dynamics and stratigraphy.

The hurricane seasons of 2004 and 2005 in the Gulf of Mexico were extremely active. Two of the major hurricanes, Ivan in 2004 (a category 3 at landfall) and Dennis in 2005 (a category 3 at

landfall), had tremendous impact along the NW Florida Barrier island coast, resulting in large-scale regional overwash deposits. Along the Florida Atlantic coast in 2004, two hurricanes, Frances (a category 2 at landfall) and Jeanne (a category 3 at landfall) affected nearly the same location within a 1 month period, and also produced extensive washover deposits. The close temporal spacing of these storms provided a unique opportunity to study the erosional and depositional characteristics of regional overwash deposits from multiple hurricanes.

The dramatic impact of overwash events on barrier-island morphology has led to considerable literature on their sedimentary characteristics. Donnelly *et al.* (2006) provided a comprehensive review of the current state of knowledge on overwash processes, deposits and modelling. Andrews (1970) documented in detail the depositional facies of a large washover fan associated with a barrier-island breach, and the erosional-depositional characteristics of overwash (or breaching) channels. Schwartz (1975, 1982) and Leatherman & Williams (1977, 1983) described detailed sedimentary structures associated with small-scale overwash deposits. Two basic bedding structures were described including horizontal to very low angle, landward-dipping stratification and steep delta-foreset bedding. Channel-related features were inferred but not directly observed. The Schwartz (1982) model has been widely used to characterize washover deposits. Morton (1978) described large-scale rhomboid bed forms associated with hurricane overwash and suggested that standing oblique waves from unidirectional nearly supercritical flow were primarily responsible for their formation. Sedgwick & Davis (2003) discussed the identification and preservation of washover deposits (mostly small scale) in the stratigraphic record. They concluded that the preservation potential of the sedimentary structures at the intertidal level and lower tends to be quite low because of active bioturbation. Hayes (1967) suggested that significant sedimentation can also occur seaward of the barrier island during the waning and draining phase of the storm surge. Most of the sedimentological studies were accomplished by trenching and coring through modern washover deposits.

Generally, overwash occurs when elevated water levels, caused by storm surge and wave runup, exceed the height of the barrier island. Direct measurement of overwash hydrodynamics is difficult. Fisher *et al.* (1974), Leatherman

(1977) and Leatherman *et al.* (1977) measured the hydraulic conditions during an overwash event caused by a weak winter storm, obtaining Froude numbers of nearly 1.

Sallenger (2000) developed an impact scale incorporating both storm and morphological parameters. Four parameters,  $D_{\text{HIGH}}$ ,  $D_{\text{LOW}}$ ,  $R_{\text{HIGH}}$  and  $R_{\text{LOW}}$ , are used to evaluate the level of morphological impact of storms.  $D_{\text{HIGH}}$  is the elevation of the highest part of the 'first line of defence' (e.g. the foredune ridge).  $D_{\text{LOW}}$  is the elevation of the base of the dune for beaches with a foredune ridge. For beaches without a foredune ridge,  $D_{\text{LOW}} = D_{\text{HIGH}}$ .  $R_{\text{HIGH}}$  and  $R_{\text{LOW}}$  are representative high and low elevations of the landward margin of swash, respectively. The first two impact scales, 'swash and collision regimes', are not associated with overwash. When  $R_{\text{HIGH}}$  is higher than  $D_{\text{HIGH}}$  but  $R_{\text{LOW}}$  is lower than  $D_{\text{HIGH}}$ , the third impact scale, 'overwash regime' occurs (Morton & Sallenger, 2003). The fourth and most severe impact, the 'inundation regime', occurs when  $R_{\text{LOW}}$  exceeds  $D_{\text{HIGH}}$ . Low-lying barrier islands are especially susceptible to inundation regime (Dingler & Reiss, 1995).

Overwash can be classified into two general groups: that which is directly related to barrier-island breaches and that which is not. Breach-related washover, such as the case described by Andrews (1970), tends to demonstrate a fan-shaped morphology with a large portion of the sediment being deposited in the intertidal zone. The processes are significantly influenced by the channelized connection of open ocean to back-barrier bay. Many times, this kind of overwash may develop into a flood-tidal delta along with the development of the breach into an inlet (Davis & Barnard, 2000). The overwash caused by Hurricane Charlie in 2004 in SW Florida is directly related to breaching (Fig. 1). The photograph shown in Fig. 1B was taken nearly 10 months after the impact. The original breach (Fig. 1A) was nearly 500 m wide. Significant spit growth from both sides of the breach has occurred, reducing the channel width to 130 m. Based on the aerial photograph (Fig. 1B), the rate of spit growth is on the order of  $1.3 \text{ m day}^{-1}$ . Depositional patterns associated with channels are apparent in the aerial photographs. The majority of deposition occurred in the intertidal zone. Barrier breaches and the associated overwash tend to occur at relatively narrow and low-lying portions of a barrier island.

Regional-scale overwash also occurs without being directly related to barrier-island breaching.

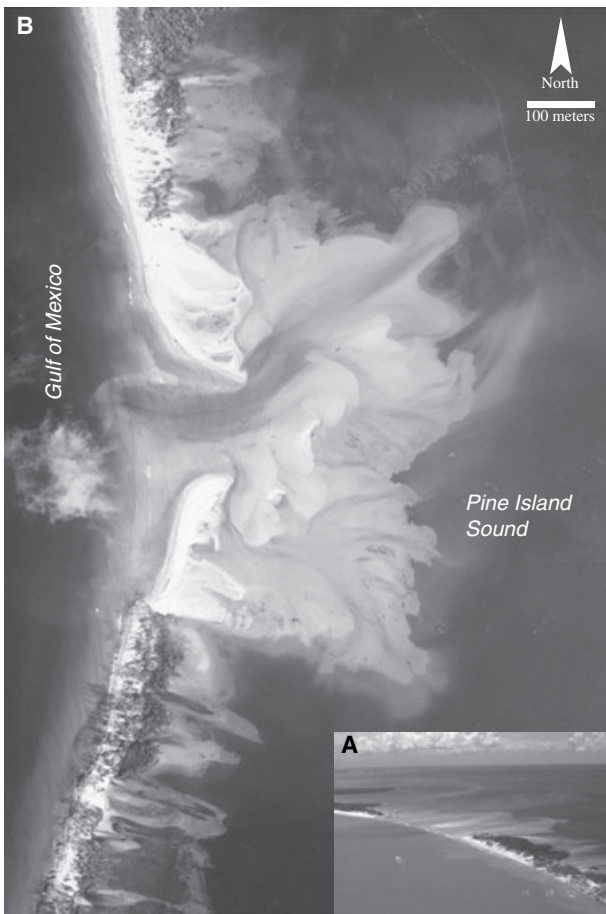


**Fig. 1.** Barrier-island breach and associated washover deposits caused by Hurricane Charlie on 13 August 2004. The breach occurred at North Captiva Island along the west-central Florida coast (see Fig. 3 for location). (A) North-looking oblique aerial photograph taken 2 days after the breaching (photograph courtesy of NASA), showing the initial 500 m wide breach connecting the Gulf of Mexico with Pine Island Sound. Washover deposition occurred largely within the intertidal zone, forming multiple overlapping shore normal washover tongues extending landward into the sound up to 1000 m. (B) Overhead aerial photograph taken 10 months after the breach. While the overall rectangular morphology of the original washover deposit has been retained, a considerable amount of sediment reworking has occurred because of wave action and channelized tidal flows. Significant spit growth, from both sides, has reduced the breach width from 500 m to 130 m in the 10 months, yielding a spit-growth rate of about  $1.3 \text{ m day}^{-1}$ . Severe beach erosion, especially along the south side, is apparent.

This happened along the northern Florida coast during hurricanes Ivan and Dennis, and to a lesser extent along the East Florida coast during Frances and Jeanne (Fig. 2). Hydrodynamics and sedimentary processes of this type of overwash can be substantially different from the breach

overwash because the connection between the open ocean and back bay, if any, is not significantly influenced by channels. A large amount of sediment is deposited above the high-tide line. This study focuses on regional scale non-breach-related overwash and the variations in process response associated with the different barrier-island sub-environments (e.g. dune field, interior marsh, interior mangrove swamp and back-barrier bay).

Recently, ground-penetrating radar (GPR) has been widely used to study near-surface sedimentary and stratigraphic characteristics. Compared with traditional trenching and coring, GPR has the advantage of much improved spatial coverage. Numerous studies have been conducted employing GPR on coastal barrier islands. Leatherman (1987) and Jol *et al.* (1996) examined various factors influencing the application of GPR within the barrier-island environment. They concluded that GPR can be used effectively on coastal barrier islands that host reasonably thick freshwater aquifers, and are composed of sediment with little to no clay or silt. Using high-resolution GPR, Dougherty *et al.* (2004) and Buynevich *et al.* (2004) identified relic dune scarps in the subsurface strata. GPR imaging provides a reliable tool for the study of sedimentary structures in both desert (Bristow *et al.*, 1996) and coastal dunes (Clemmensen *et al.*, 2001; Botha *et al.*, 2003). As overwash deposits are closely associated with dune erosion, it is important to understand the internal structure of sand dunes. Using GPR imaging, Møller & Anthony (2003) concluded that the stratigraphy of a transgressive coastal barrier along the Danish North Sea coast is largely composed of washover deposits, suggesting that overwash and the resulting washover deposits could contribute significantly to barrier-island stratigraphy elsewhere. This conclusion is not surprising given the fact that overwash provides a major mechanism for the landward movement of sediments.

The objective of this study was to characterize erosional and depositional features from multiple regional overwash events in some of the key barrier-island sub-environments including the dune field, interior wetland and back-barrier bay. Data from trenches, cores and GPR profiles are included. These data should provide valuable insight into identifying ancient washover deposits, quantifying washover volumes, depicting overwash processes, thereby improving understanding of barrier-island processes and stratigraphy.

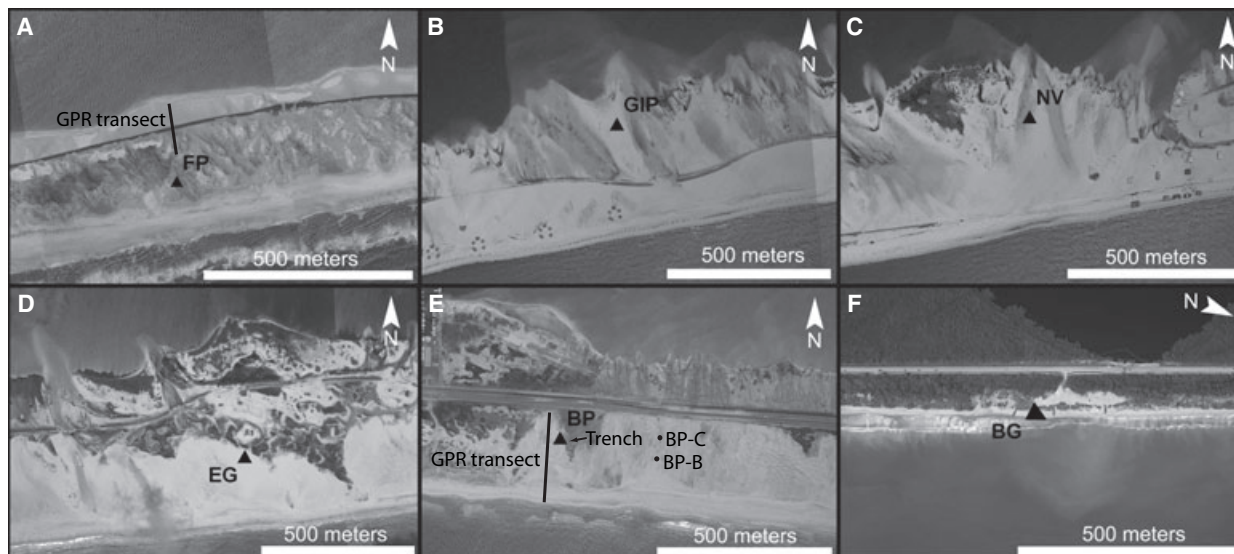


**Fig. 2.** Regional-scale overwash at the six study sites. The five Gulf-facing northern Florida sites, located on Santa Rosa Island are shown from west to east in photographs A to E (FP – Fort Pickens; GIP – Gulf Breeze National Seashore; NV – Navarre Beach; EG – Eglin Air Force Base; BP – Beasley Park). Photograph F shows the Atlantic-facing east coast site (BG – Bob Graham Park). Photographs A to E illustrate the transition from washover extending into the back bay (A to C) to washover largely confined to the subaerial portion of the barrier island (D and E). The locations of GPR transects, pound cores (BP-B, BP-C), and trenches (black triangles) shown in the following figures are also indicated here. Photographs A to E were taken on 11 to 13 July 2005 (post-Dennis), and photograph F on 26 September 2004 (post-Jeanne) by NOAA. Site locations are shown in Fig. 3.

## STUDY AREAS

The current study was conducted along two discrete stretches of Florida coastline (Fig. 3). Hurricanes Frances and Jeanne both made landfall at nearly the same location on Hutchinson Island along the Florida Atlantic coast in September 2004. Hurricanes Ivan in 2004 and Dennis in 2005 caused extensive overwash along the NW Florida Panhandle coast. The study areas were chosen based on: (i) proximity to storm centre, (ii) a paucity of anthropogenic modification, and (iii) locations representing a range of barrier-island sub-environments, morphology and sediment characteristics.

The SE coast of Florida is oriented roughly north–south along the Atlantic Ocean. The study site, Bob Graham Park (BG), is located on Hutchinson Island (Figs 2F and 3D), a 35 km long barrier island ranging in width from 0.2 to 2.0 km. The monthly average significant wave height ranges from 1 to 2 m, and the mean tidal range is 0.8 m. BG is situated 5 km north of the landfall of Frances and Jeanne. While much of Hutchinson Island is heavily developed, the study area lies within an undeveloped recreational area, characterized by dense mangrove swamp lying landward of the beach and narrow low dunes (Fig. 2F). The sediment varies greatly in size and texture with a

high concentration of shell debris. An average of 80 samples yielded a  $\text{CaCO}_3$  concentration of 65%.

The northern coast of Florida, the Florida Panhandle, presents a different environment in contrast to the Atlantic coast. The coastline is oriented roughly east–west along the Gulf of Mexico, with a tidal range of <0.5 m (Morang, 1992). The significant wave heights average *ca* 1.2 m during the winter months and 0.8 m during summer. The Panhandle study sites are located on Santa Rosa Island, a 73 km long barrier island lying within the Gulf of Mexico, and backed on the north by Santa Rosa Sound (Fig. 3).

In contrast to the densely mangrove-covered east coast study site, Santa Rosa Island and the Panhandle study sites (Fig. 2A–E) are characterized from bayside to Gulf by: (i) high interior dunes covered with mature woody vegetation; (ii) patchy ephemeral intra-dune wetlands and grassy marsh, (iii) broad interior platforms with low dunes and sparse grassy vegetation, and (iv) high semi-continuous frontal dunes populated with sea oats, which merge seawards with the back-beach. Sediment is compositionally and texturally homogeneous with over 98% of the sediment being comprised of quartz sand, 75% of which lies within the 0.2 to 0.4 mm grain-size fractions (Stone & Stapor, 1996). Shell-debris content is low, rarely exceeding 5%. An average of 10

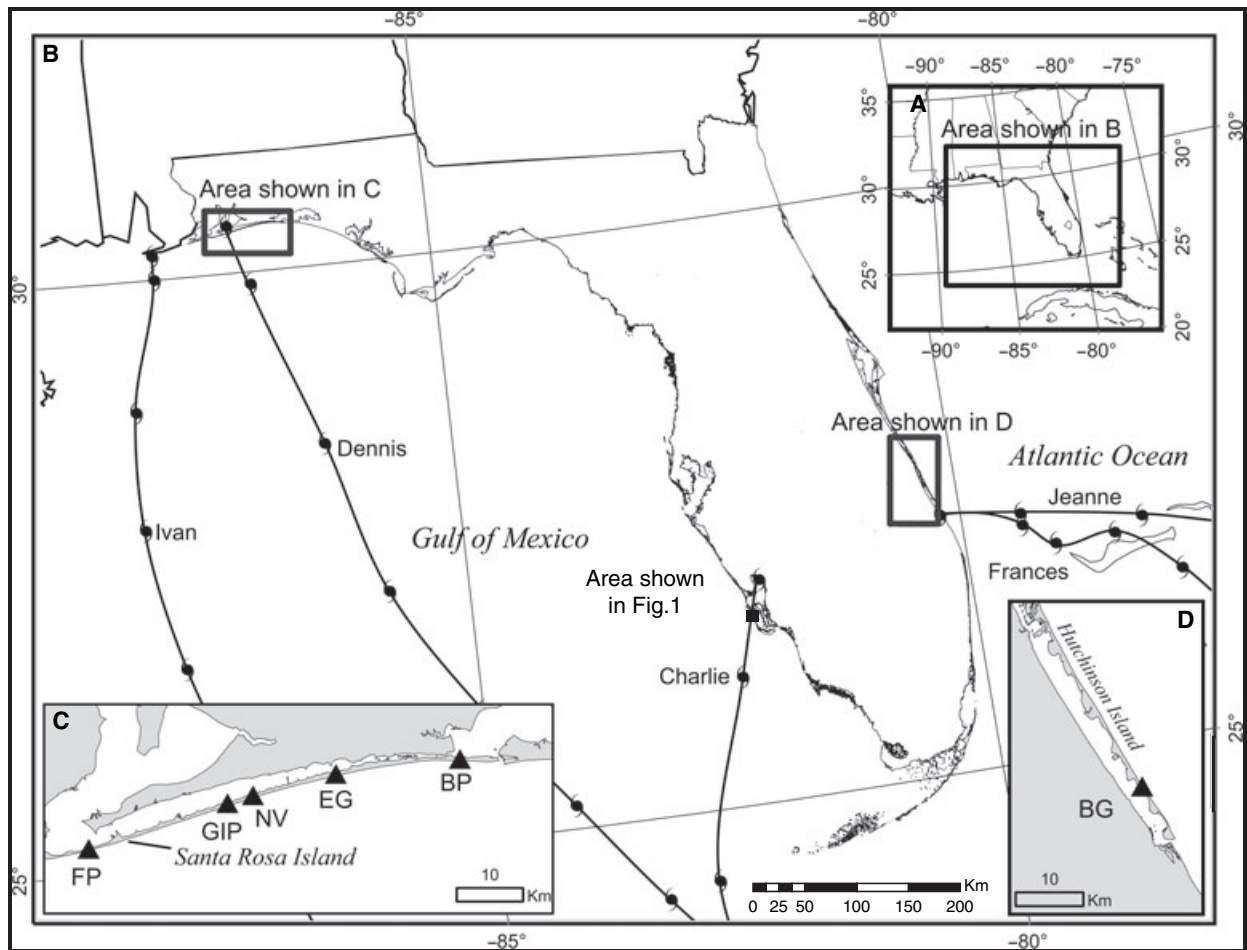


**Fig. 3.** Location map of study areas. (A) Map of SE United States. (B) Map of Florida showing the study areas (rectangular outlines), and the tracks of the studied hurricanes. With the exception of the hurricane landfall positions, the hurricane icons represent hurricane centre positions at 6-h intervals. (C) Map of Santa Rosa Island and the Panhandle study sites shown in Fig. 2A–E. (D) Map of the southern portion of Hutchinson Island with the Atlantic-facing Bob Graham Park (BG) study site shown in Fig. 2F.

samples yielded a  $\text{CaCO}_3$  concentration of 2%. A small amount of heavy minerals (Stapor, 1973) tend to concentrate in the 0.1 to 0.15 mm grain-size fraction in thin layers and laminae (Horwitz & Wang, 2005), and provide a basis for distinguishing stratification.

Hurricane Ivan induced dramatic morphological and sedimentological changes along the Florida Panhandle coast. Inundation and regional overwash occurred within 100 km from the storm centre at landfall. Substantial beach and dune erosion was measured as far as 300 km east of the storm centre. The highest elevation of beach erosion extended considerably above the measured storm-surge level, indicating that storm-wave setup and swash runup played essential roles in controlling the elevation of beach erosion (Wang *et al.*, 2006). An erosional surface was observed along the foredune and backbeach,

extending over 300 km eastward from the storm centre. A storm layer of up to 50 cm thick was deposited above the erosional surface.

The five Panhandle study sites (Figs 2 and 3), spanning *ca* 60 km of coastline, include from west to east, Ft. Pickens Park (FP), Gulf Breeze (GIP), Navarre Beach (NV), Eglin Air Force Base (EG) and Beasley Park (BP). The westernmost FP site was largely inundated by Ivan, with very few dunes surviving. This site is located to the west of the Dennis landfall. The GIP site was also inundated by Ivan and lies at the landfall position of Dennis. The NV site is situated within the transition zone from inundation to overwash, with many of the larger dunes surviving. The EG site was dominated by overwash and most of the landward dunes survived. Overwash did not extend into the backbay (Santa Rosa Sound) at most places. The easternmost BP site is in the

transition zone from overwash to collision regime, with extensive dune scarping. Overwash occurred in areas with low dunes.

### WAVE AND TIDE REGIMES ASSOCIATED WITH HURRICANES FRANCES, IVAN, JEANNE AND DENNIS

During the passage of hurricanes Frances and Jeanne, National Data Buoy Center (NDBC) station 41009, located *ca* 130 km north of the landfall site was the closest functioning wave gauge. The highest wave measured was 7.5 m just before the landfall (Fig. 4). A surge of nearly 1 m was measured *ca* 100 km north of the landfall. The surge closer to landfall is expected to be much higher, as supported by visual evidence, such as the elevation of debris lines and sand levels in lower housing units. The elevated water levels persisted for more than 30 h during Frances and 20 h during the faster-moving Jeanne.

Ivan, a large sustained category 4 hurricane that weakened to a strong category 3 at landfall, came

onshore with extreme wind, wave and surge. Figure 5 shows the measured wave and surge conditions as the hurricane approached the coastline. The selected tide gauges are close to the open Gulf, and therefore should provide reliable surge measurements. At Ivan landfall, sustained hurricane force winds extended 170 km from the centre. Most of the overwash occurred within this zone. Sustained tropical storm strength winds extended 475 km from the centre.

Significant and sustained surge was measured over a large area during the passages of both Ivan and Dennis (Fig. 5). At the Pensacola tide gauge, the highest surge measured was 2.1 m above the mean low low water (MLLW) for Ivan and 1.5 m for Dennis. The capacity of the gauge was exceeded at Ivan landfall. Many qualitative pieces of evidence indicate that the water level substantially exceeded the 2.1 m mark (Wang *et al.*, 2006). This tide gauge is located to the west of the Dennis landfall. Dominated by offshore winds, the water level measured inside Pensacola Bay may not be representative of conditions on

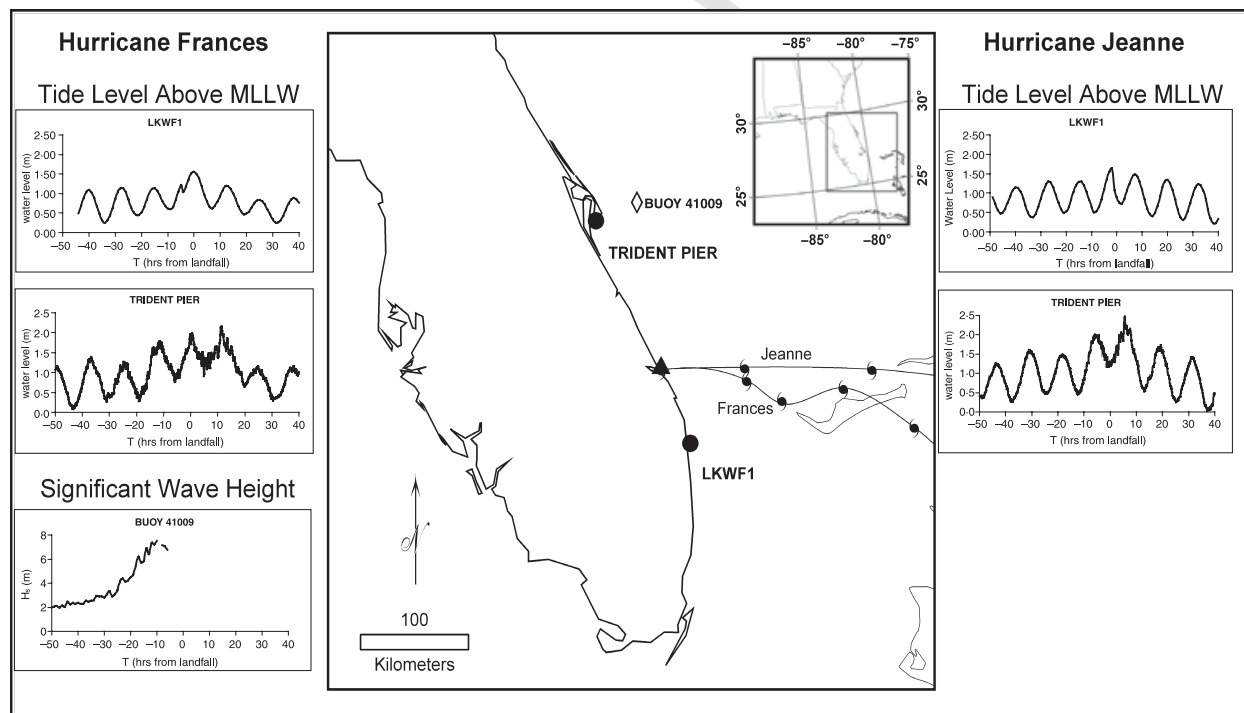


**Fig. 4.** Map of peninsular Florida (centre panel) showing the locations of tide gauges (solid circles), offshore wave buoy 41009 (diamond), the tracks of hurricanes Frances and Jeanne, and the Bob Graham (BG) study site (solid triangle). The left panel shows water levels and significant wave heights measured during the passage of hurricane Frances. The right panel shows water levels during the passage of hurricane Jeanne. Buoy 41009 was damaged by Frances and remained inoperable during Jeanne. Zero hour on the horizontal axis represents the time of landfall. It should be noted that the tide gauges and wave buoy are located considerable distances from the hurricanes landfall positions and the study site.

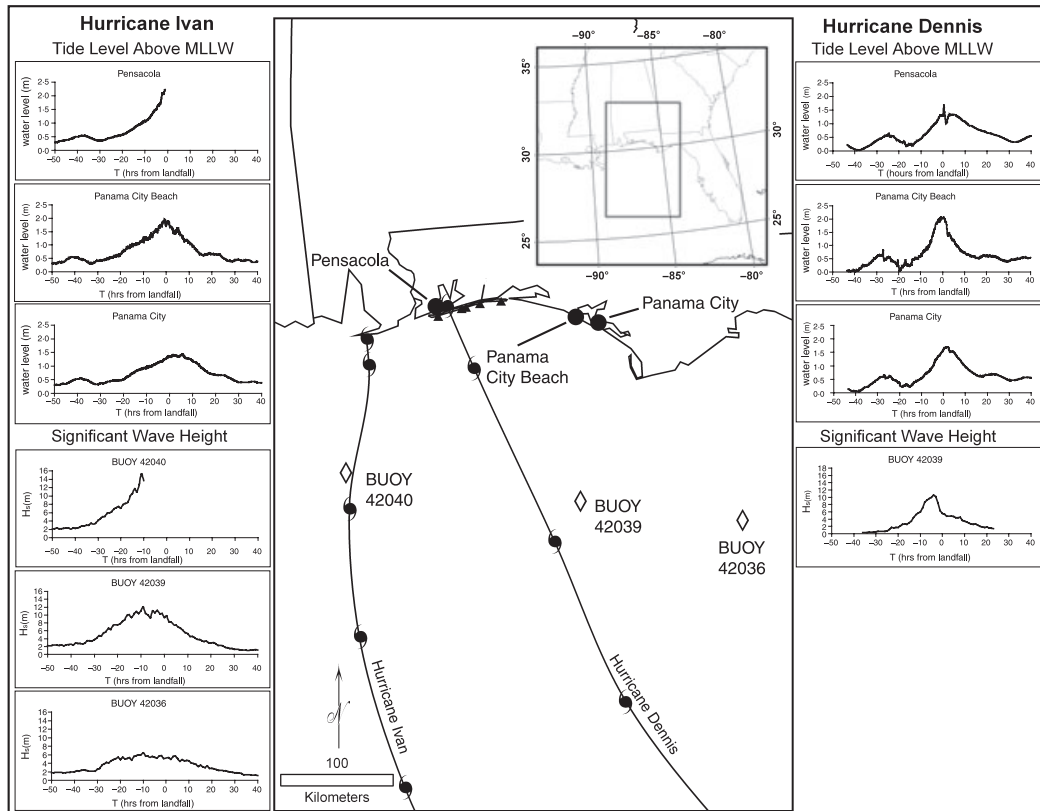


**Fig. 5.** Map of the Florida Panhandle (centre panel) showing the locations of tide gauges (circles), offshore wave buoys (diamonds), the tracks of hurricanes Ivan and Dennis, and the Panhandle study sites (triangles). The left panel shows water levels and significant wave heights measured during the passage of hurricane Ivan. The right panel shows water levels and significant wave heights measured during the passage of hurricane Dennis. Wave buoys 42040 and 42036 were not in operation during the passage of Dennis. Zero hour on the horizontal axis represents the time of landfall.

the Gulf side. At Panama City Beach, near the east boundary of the study area, the tide gauge is located along the Gulf beach. The highest surge measured was 2.0 m above MLLW during both Ivan and Dennis, nearly four times the typical tidal range. Surge levels above 1.5 m (MLLW) persisted for over 10 h (Fig. 5).

Extremely high waves were measured at the NDBC wave buoys. Shortly before the Ivan landfall, 16 m waves were measured at the westernmost gauge 42040 (Fig. 5), which damaged the gauge. At gauge 42039, 220 km to the west, the highest wave was 12 m. Further east at gauge 42036, the highest wave was 6.4 m. The highest waves at all three buoys were measured shortly before landfall. These extreme offshore wave conditions lasted through the landfall. The high waves generated by Hurricane Ivan offshore Pensacola exceeded historical records (Stone *et al.*, 2005). Wang *et al.* (2005) measured higher waves than those reported by the NDBC buoys, with maximum wave height ( $H_{\max}$ ) reaching 30 m near

the Ivan centre. The highest waves measured during the passage of Dennis were *ca* 10 m high. The forward speed of Dennis was much greater than that of Ivan. This is reflected in the narrower peaks in the wave and surge data.

It is worth emphasizing that the surge levels measured (Figs 4 and 5) do not include the wave setup and swash runup that occur along open beaches. Based on beach-profile changes, Wang *et al.* (2006) found that the wave setup and swash runup accounted for 50% of the total elevated water level during the impact of Ivan. Therefore, wave setup and swash runup should contribute significantly to the overwash processes and deposition.

## METHODOLOGY

Coring, trenching and GPR imaging were used to investigate the erosional and depositional characteristics of overwash caused by the multiple

storms. Overall, 78 cores, 21 trenches and *ca* 60 km of GPR profiles were collected. The field data collection was conducted within 8 months after the storm impacts, before the next summer. Prestorm and poststorm beach profiles were surveyed at the BP site, allowing exact quantification of washover-sediment volume along the profile.

Sediment cores were collected by driving a 7.6 cm diameter aluminum pipe into the subsurface with a sledge hammer. Using this procedure, cores can be obtained up to 2 m below surface. Similar procedures of core description and sampling as used by Sedgwick & Davis (2003) were used here. Trenches of various shapes (e.g. T- or L-shape) and sizes (up to 6 m long and 1.5 m deep) were excavated to examine the stratigraphy and sedimentological aspects of the washover deposits in detail. GPR transects were adjacent to selected trenches. Trench and core data were used to ground truth the GPR data.

While traditional trenching and coring techniques provide valuable insight into the detailed sedimentological characteristics of unconsolidated sediments, these methods are limited in spatial coverage. GPR is a non-invasive geographical technique widely employed in sedimentological studies to increase spatial coverage. The principles of GPR are discussed in detail by Daniels *et al.* (1988) and Davis & Annan (1989).

The GPR profile data were collected using a Sensors and Software Noggin SmartCart (Sensors and Software Inc., Mississauga, Canada), equipped with a 250 MHz antenna and 100 V transmitter. A PulseEKKO 100 with a 200 MHz antenna and 400 V transmitter was employed for common midpoint (CMP) gathers. SmartCart data were collected in common offset mode with the antenna separation fixed at 0.3 m, using a 0.05 m step size. Transect locations were established with a WAAS-enabled GPS, and the transects were surveyed for topographic control. The GPR data were processed using Sensors and Software EKKO Mapper software. All data were dewowed and scaled. Given that imaging continuity of stratigraphic horizons and sedimentary structures were the primary objectives of the GPR survey, maximum gain and pulse width settings of 400 and 1, respectively, were employed. While relative amplitude information is lost in this process (e.g. contrast between high- and low-amplitude reflections), lower-amplitude reflections are enhanced, thereby allowing better imaging of sedimentary structures. CMP gathers conducted at the NV, EG and BP sites yielded average signal travel velocities of 0.12–0.13 m ns<sup>-1</sup> in the unsaturated

sands, and 0.06 m ns<sup>-1</sup> for the saturated sands below the water table. These velocities were used in the GPR interpretation, and depth scales were adjusted accordingly in order to account for the varying signal travel velocities above and below the water table. Based on the above signal travel velocities, and a nominal centre transmitting frequency of 250 MHz, vertical resolution should be on the order of one-quarter of a wavelength (Sheriff, 1977), or *ca* 0.06 m below the water table and 0.12 m above.

At the Panhandle study sites, signal penetration was on the order of 2 m, largely attributed to the significant freshwater aquifer present on Santa Rosa Island. Overall data quality was good and resolution was sufficient to image detailed sedimentological features observed in the cores and trenches. Conversely, at the east coast study site, the absence of a freshwater aquifer and shallow brackish groundwater on Hutchinson Island yielded rapid signal attenuation and generally poor-quality GPR data.

Radar reflection profiles were interpreted following the techniques and terminology described by Neal (2004). The configuration and continuity of reflections provided the basis for establishing: (i) radar surfaces, interpreted to represent depositional breaks and/or washover unit contacts, and (ii) radar facies, interpreted to represent sedimentary structure within the washover deposits. Interpreted profiles were compared with sedimentological features observed in cores and trenches. The present study is focused on the sedimentary characteristics of the recent washover deposits. Sedimentary units lying below the storm layer were not examined in detail.

## RESULTS

The main purpose of this paper is to examine and generalize the erosional and depositional characteristics associated with regional-scale overwash, emphasizing the variations in barrier island process response as a function of morphologic and biological conditions. Therefore, the following discussion is mostly based on specific features and their associated processes, summarized from numerous examples. Spatial distribution of these features is discussed in a general fashion with only limited reference to specific locations. Regional morphological and sedimentological controls are also discussed, comparing the overwash along the northern Gulf and southern Atlantic coasts.



## Overwash into dune field

Overwash into a dune field may take two forms. If the storm is relatively weak and the dune field is high and well established with dense vegetation, localized and small-scale overwash occurs within the dune field. If the storm is extremely powerful, the dune field may suffer tremendous erosion and be largely replaced by an overwash platform. The latter occurred extensively along the Florida Panhandle coast during the 2004 and 2005 hurricane seasons and is the focus here.

Hurricane Ivan caused tremendous dune erosion, spanning from the frontal-active dunes with grass-type vegetation to the interior inactive dunes with mature woody (e.g. scrub oak) vegetation. A significant portion of the dune field was replaced by a washover platform. The erosional surface between the washover deposit and the eroded densely vegetated inactive dunes is easily identifiable in trenches (Fig. 6A). The underlying sediment has a much higher organic concentration and contained substantial residual root material. The relic root system extended into the washover deposits and in places was exposed at the surface. The contrasting sediment composition (e.g. organic content) along the boundary returned prominent reflections within GPR profiles (Fig. 6B and C). Numerous discrete hyperbolic reflections observed within the GPR data represent large woody stem and root material. The washover deposits are characterized by horizontal bedding.

The boundary between the washover deposits and the eroded active, sparsely vegetated dunes is distinguishable but not as sharp as the case discussed above. The washover deposits were well defined by prestorm and poststorm surveys at the BP site (Fig. 7). In the cores, the washover sediment is characterized by heavy mineral-rich horizontal layers and laminae, and is easily distinguished from the underlying bioturbated sediment. As discussed by Sedgwick & Davis (2003), the preservation potential of laminations and the basal boundary tends to be low due to bioturbation. However, in places where the washover layer is thick, e.g. over 1 m, the sedimentary structures in the lower portion and the basal contact may have a higher preservation potential.

Ground-penetrating radar profiling allows the imaging of sedimentary structures over a much larger section than trenches. This provides the possibility of identify large-scale features that cannot be depicted from trenches. Figure 8 shows a 270 m shore-perpendicular GPR profile extend-

ing from the high-tide line (left-hand side of Fig. 8) landward into the barrier-island interior. A truncated dune was identified in the GPR profiles near the Gulf side. Landward of the truncated dune, slightly landward-dipping bedding was identified. The sub-horizontal bedding merges landward into steeply dipping tabular foreset bedding as the overwash lobe progrades into the interior marsh.

A trench was dug in the vicinity of the GPR profile referred to above, near the landward end of a washover lobe. A sharp boundary was identified at the bottom, with much more organic content beneath representing older bioturbated sediment (Fig. 9). Above the sharp contact, there is a layer of slightly bioturbated sand, *ca* 50 cm thick. This layer may represent the washover deposited by Hurricane Opal in 1995, the last significant hurricane to impact the Panhandle before Ivan in 2004. It is also possible that this layer represents small interior dunes near the edge of an interior marsh wetland. The Ivan washover deposit is roughly 40 cm thick. Rapid sedimentation is apparent as indicated by buried marsh grass.

Comparing the above trench (Fig. 9) with the GPR profile (Fig. 8), it is apparent that each method has advantages and disadvantages. Trenching, while providing limited spatial coverage, reveals detailed sedimentological information, such as degree and characteristics of bioturbation and overwash by multiple storms. The GPR profile can demonstrate larger-scale features, such as truncated dunes, as well as broader sedimentological trends and patterns.

It is reasonable to deduce that the extensive erosion and 'wiping out' of dunes are dominated by wave action. This is consistent with the findings of Wang *et al.* (2006) that wave setup and swash runoff, in addition to storm surge, contribute significantly to an elevated storm water level. The wave forcing is also attributable to the formation of the flat overwash platform and the associated horizontal bedding. Oscillatory motion in shallow water, such as swash, is associated with large Froude numbers and tends to generate planar bedding. With the extremely strong onshore wind, extensive surf bores should be expected as the water level rises over the barrier island.

As a result of the short time (10 months) between Ivan and Dennis for the development of bioturbation features, it is difficult to separate Dennis washover from Ivan deposits. At some study sites, e.g. the BP site, variations of heavy

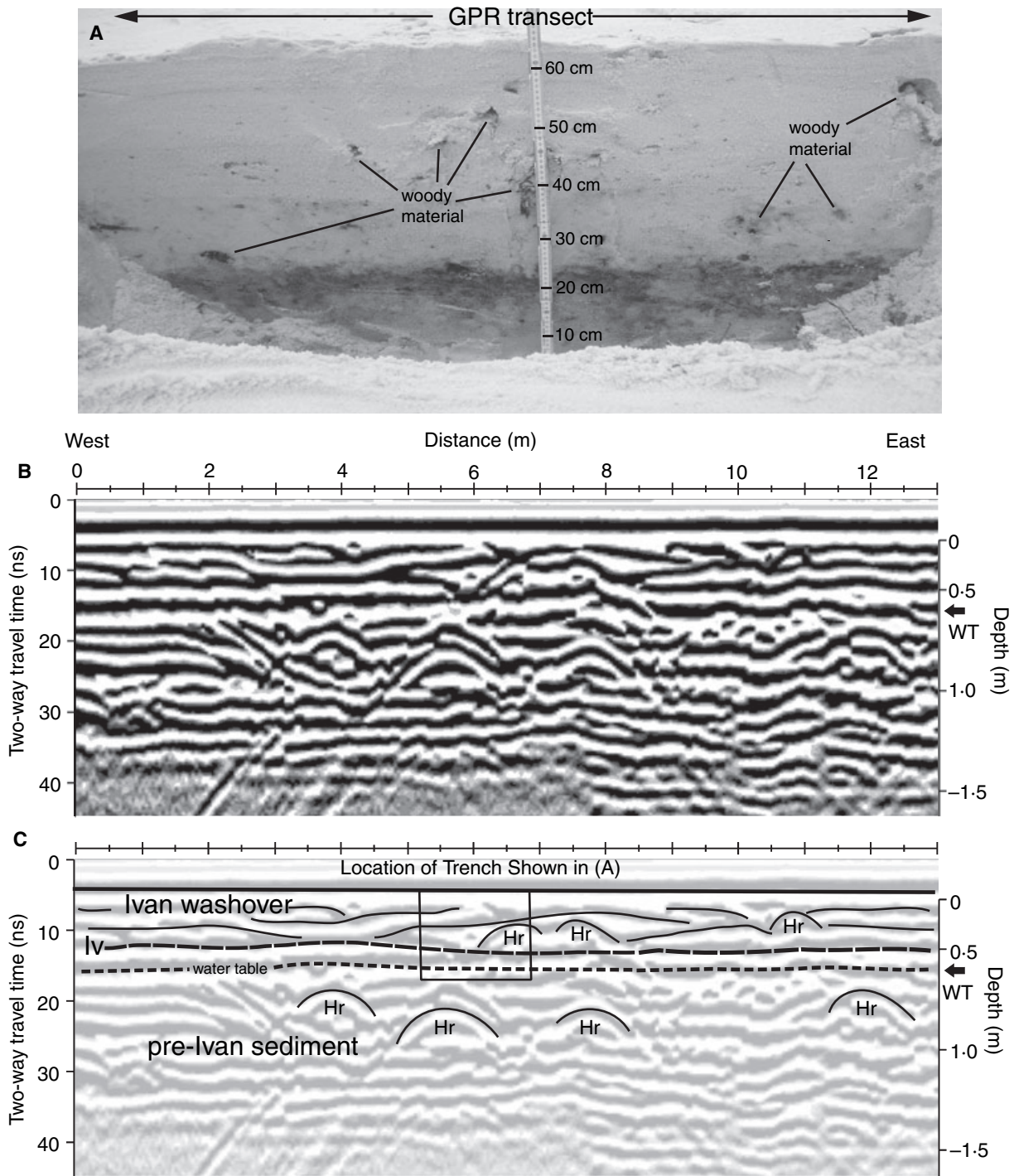


**Fig. 6.** (A) Trench excavated at the NV study site (see Fig. 2C for an aerial view). The trench was excavated post-Ivan and pre-Dennis. The base of Ivan washover is marked by the sharp contact near the floor of the trench separating the light coloured Ivan washover deposit from the underlying dark organic-rich sediment. Coarse tree branches and roots entrained within the washover sediment are exposed in the trench wall. (B) 250 MHz GPR profile scanned adjacent to the trench. The depth conversion is based on a velocity of  $0.12 \text{ m ns}^{-1}$  above the water table and  $0.06 \text{ m ns}^{-1}$  below the water table. (C) Line-drawing interpretation of the GPR profile showing, the radar surface Iv, interpreted as the bottom boundary of the Ivan washover; the position of the water table (WT) below Iv, and numerous discrete hyperbolic reflections (Hr), both within Ivan washover and below, caused by the coarse wood material. The black box outline corresponds to the trench shown in (A).

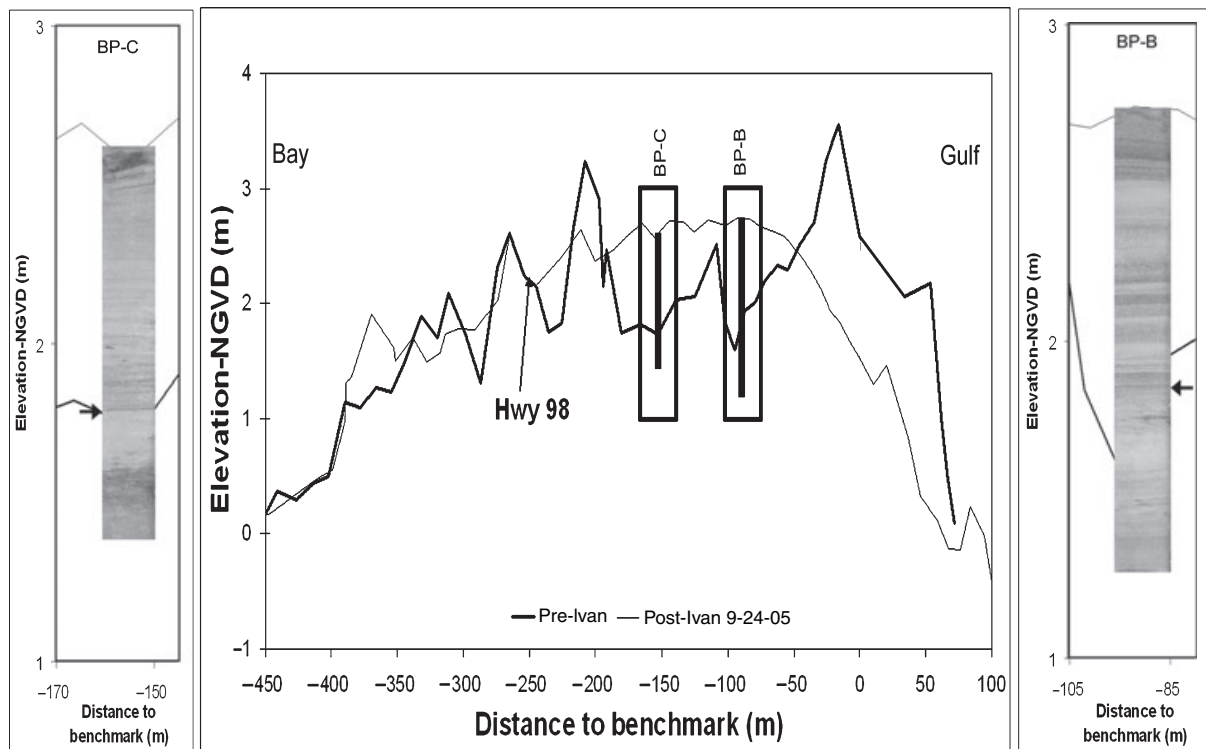


**Fig. 7.** Pre-Ivan and post-Ivan cross-island profiles from the BP study site (Fig. 2E), and associated pound cores. The profiles (centre panel) illustrate the extensive erosion along the backshore and foredune between  $-50$  m to  $75$  m (distance to benchmark), and washover deposition in the barrier interior (overwash platform) between  $-190$  m and  $-50$  m. The right and left panels show photographs of cores BP-B and BP-C collected along the profile. The base of Ivan washover is indicated by the arrows. Dark banding in the washover sediment is attributed to heavy mineral-rich laminae. The thickness of Ivan washover unit as measured in the cores ( $0.8$ – $0.85$  m) correlates well with the prestorm and poststorm survey data.

mineral lamination thickness and clustering may provide some hints, but cannot be used as solid evidence.

### Overwash into the wetland in the barrier-island interior: the role of vegetation

Two different types of interior wetland environment are investigated in this study: (i) marsh along the Panhandle coast, and (ii) mangrove swamp along the southern Florida Atlantic coast. Different interactions between overwash and vegetation are expected from the two environments. In addition, the sediments at the two sites are very different in terms of grain size, texture and composition.

Along the Florida Panhandle barrier islands the washover deposits within the interior marsh demonstrate steep tabular foreset bedding (Fig. 10), as described in many previous studies (e.g. Schwartz, 1975). Figure 10 also demonstrates that GPR imaged the sedimentary structure well. A sharp contact is apparent at the bottom of

the washover deposit. Buried marsh grass, relatively fresh and still upright, provided good evidence of rapid washover deposition. The Ivan washover layer is nearly  $1.2$  m thick at this location.

A trench was dug slightly landward (toward the marsh) of the above trench following Hurricane Dennis in order to examine washover deposits resulting from multiple storms (Fig. 11). Consistent with earlier observations, a sharp boundary with buried marsh grass was observed at the base of Ivan washover. A thin ( $3$ – $4$  mm) algal mat layer was observed at the landward edge of the trench. This layer separates the Ivan and Dennis deposits. Algal mat layers are often regarded as good boundaries for washover deposits (Sedgwick & Davis, 2003). The algal mat pinches out upward and seaward, limited by the increased elevation to above the ponding level (Fig. 11D). A subtle angular discontinuity extends seaward from the terminal end of the algal mat further representing the boundary between the Dennis and Ivan washover deposits. It is worth noting that the

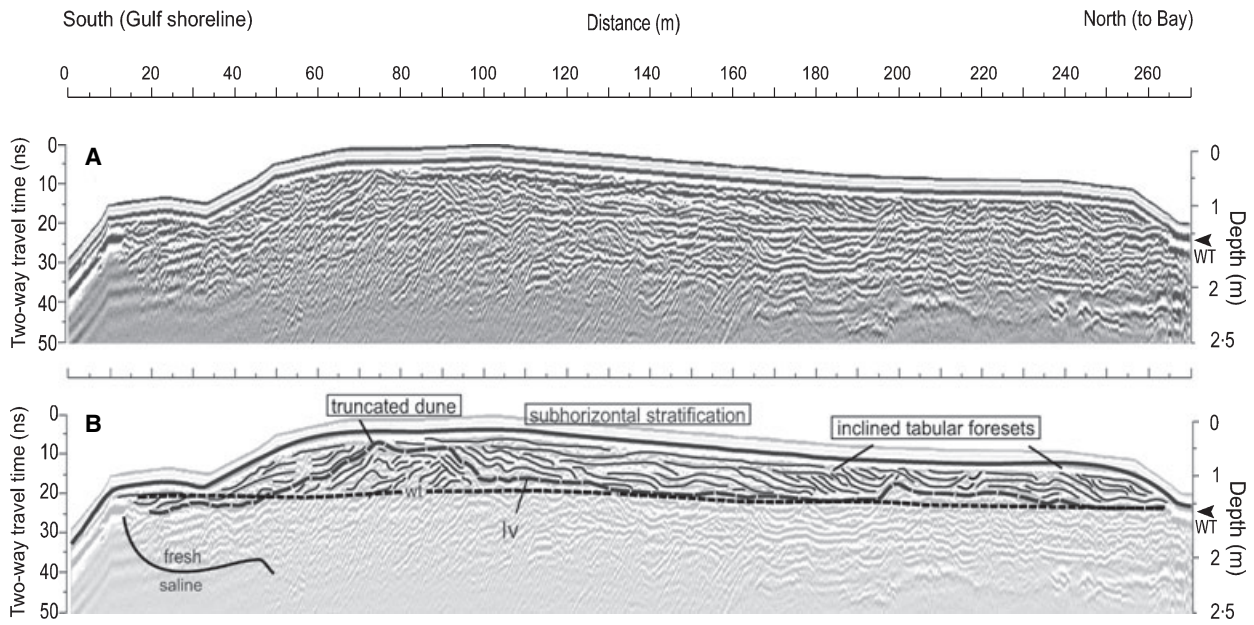


**Fig. 8.** (A) 250 MHz GPR transect scanned over hurricane Ivan washover deposit at the BP study site (Fig. 2E). The transect, scanned post-Ivan and pre-Dennis, is oriented shore normal and extends from the Gulf of Mexico shoreline (left edge) landward to the terminal end of the washover lobe. The depth conversion is based on a velocity of  $0.12 \text{ m ns}^{-1}$  above the water table, and  $0.06 \text{ m ns}^{-1}$  below. (B) Line-drawing interpretation of the GPR profile illustrating: (1) the position of the water table (wt), (2) radar surface Iv, interpreted to represent the base of the Ivan washover deposit, (3) bi-directional inclined reflections between 70 and 90 m representing a truncated dune, (4) subhorizontal reflections characteristic of washover deposit over the barrier interior platform, and (5) inclined reflections associated with inclined tabular foreset bedding formed as the washover prograded landward into the low-lying interior portions of the barrier island (e.g. ponds, marsh wetland).

location of this particular trench was carefully chosen to study the Dennis impact. As a result of the short time between Ivan and Dennis washover events and the homogeneity of the sediment, the boundary between the Ivan and Dennis deposits could not be recognized in other trenches or GPR profiles.

Overwash into the dense mangrove swamp is substantially different from the marsh overwash. The dramatic interactions between wind-wave-current and the dense mangrove trees are evident, demonstrated by the numerous broken, tilted and partially buried trees (Fig. 12). The landward extent of washover deposition is apparently related in part to the density of the vegetation. In places where the mangrove is less dense, the washover lobe extended further into the swamp. Moreover, a dyke made of broken plant limbs and brush often marks the landward terminus of the lobe, indicating the limiting effects of the mangrove on the overwash process.

As a result of the dense vegetation and complicated root system, trenching through washover deposits in the mangrove environment was not

productive. Moreover, the brackish water limited the GPR signal penetration to  $<1 \text{ m}$ . The sedimentological characteristics were therefore examined mostly from cores. A sharp boundary separates the organic-rich mangrove swamp deposits from the shelly washover units (Fig. 13). The organic concentration of the underlying pre-overwash sediment ranged from 2% to 24%. The Frances and Jeanne overwash events are represented by two cycles of graded bedding, both normal (ng) and reversed (rg), evident in most of the cores. The two overwash events are also indicated by the overlapping washover sediment layers (Fig. 12). The normal graded bedding tends to distribute seaward of the vegetation line, while the reversed graded bedding tends to distribute landward. This suggests that the vegetation had substantial influence on selective sediment transport and deposition. Graded bedding was not found in the Panhandle washover deposits, partly controlled by the homogeneity of the sediment grain size. The horizontal bedding and steep foreset bedding common within the Panhandle washover were not apparent in the sediment at the Atlantic BG site.

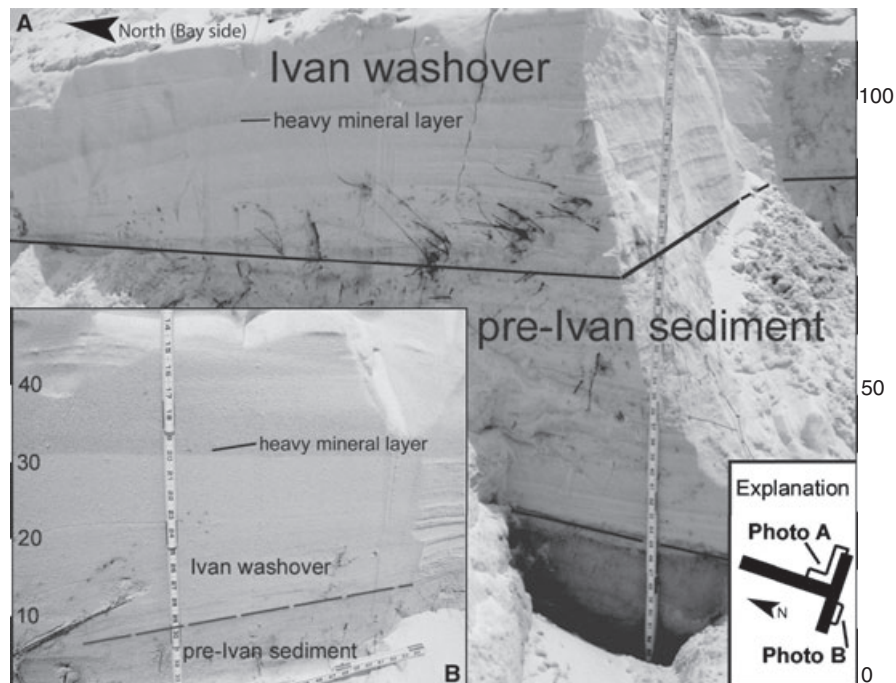


**Fig. 9.** (A) T-shaped trench excavated through Ivan washover deposit at the BP study site (Fig. 2E). The trench was excavated post-Ivan and pre-Dennis; near the eastern terminus of the washover lobe. The base of Ivan washover deposit is marked by the freshly buried grasses, inclined in the dominant overwash flow direction (north), with little evidence of scouring along the contact. Dark heavy mineral-rich laminae and an absence of bioturbation characterize the Ivan washover, while the underlying sand exhibits varying degrees of bioturbation. Near the base of the trench (photograph A), a sharp planar contact separates light coloured bioturbated pre-Ivan sediment (upper layer) from an underlying darker sand unit. This contact represents an earlier overwash event, probably associated with the passage of hurricane Opal (1995). The bar scales along the margins of the photograph are in centimetres.

The above contrasting sedimentary structures indicate different interactions between the overwash and the specific coastal environments. The dense mangrove may impose tremendous obstruction to the overwashing currents and waves, disrupting the flow patterns and resulting in extreme turbulence and sediment mixing. The planar and steep tabular bedding should result from the dominant bedload transport, while the graded bedding should be deposited mostly from suspended load induced by the intense interaction between the flow and dense mangrove.

### Overwash into the back-barrier bay

The extremely powerful hurricane Ivan caused tremendous overwash into the back-barrier bay at the two westernmost Panhandle study sites, as shown by the prestorm and poststorm aerial photographs (Fig. 14). Steep foreset bedding similar to that observed in the interior marsh is also identified within the washover deposits in the back bay. However, the back-bay washover is much thicker than that in the other sub-environments, 1.5–2.0 m vs. 0.5–1.2 m. This is largely

attributed to the increased accommodation space associated with the back bay. Moreover, the steep inclined bedding is more sigmoid-shaped than tabular. The thick back-bay washover could not be penetrated by trenching (limited in depth by the water table); however, the GPR profiles suggest a tangential basal contact (Fig. 14).

The morphological characteristics of the bay-side beach along the Panhandle coast include a narrow and steep shoreface and a shallow platform (typically <1.5 m deep) extending up to several hundred metres into the bay (Armbruster, 1997; Stone *et al.*, 2004). This platform, also referred to as a low-tide terrace (Nordstrom, 1992; Nordstrom & Roman, 1996), is common along estuary beaches worldwide. The GPR imaged the above estuary beach morphology underneath the prograding washover deposits (Fig. 14). The washover platform extending into the back bay is roughly 1.0 m above mean sea level. This, combined with the 1 m deep bay platform, resulted in a washover layer roughly 2 m thick.

The hydrodynamic conditions in the relatively open back bay should be quite different from those of the interior marsh. Considerable wave

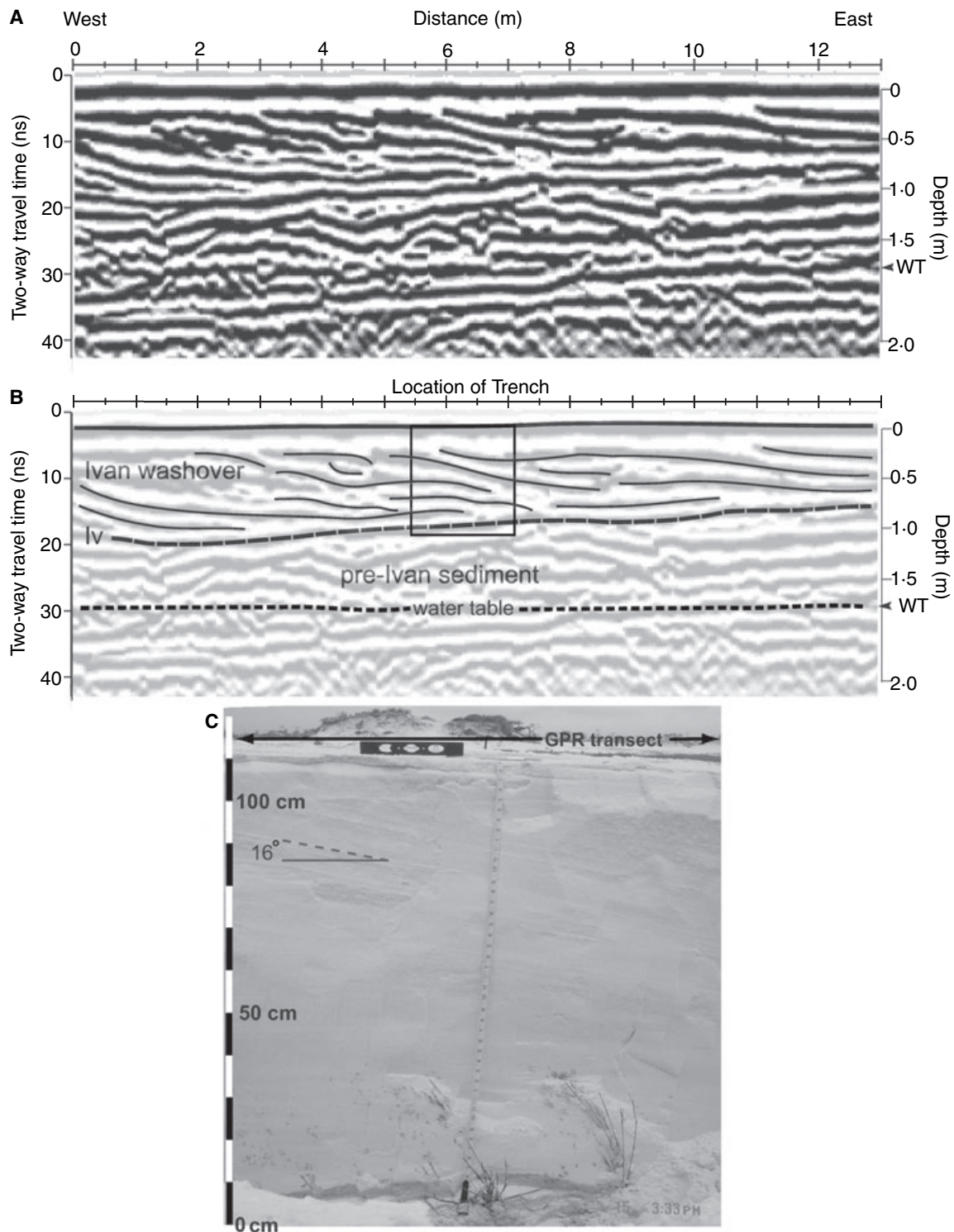


**Fig. 10.** (A) 250 MHz GPR transect scanned at the EG study site (Fig. 2D) post-Ivan and pre-Dennis, adjacent to the north wall of the trench shown in the lower photograph (panel C). The depth conversion is based on a velocity of  $0.12 \text{ m ns}^{-1}$  above the water table and  $0.06 \text{ m ns}^{-1}$  below. (B) Line-drawing interpretation of the profile showing the radar surface Iv, interpreted as the bottom of Ivan washover, and the position of the water table (WT) below Iv. The Ivan radar facies (labelled Ivan washover) is characterized by steep downlapping reflections. The black box outline corresponds to the trench. (C) Trench excavated through the Ivan washover unit. The base of Ivan washover layer is marked by freshly buried grass, and an abrupt change in sediment colour. Little evidence of scouring can be found along the contact. Stratification within the Ivan washover is inclined to the east at an apparent angle of  $16^\circ$ . The inclined stratification and basal contact exposed in the trench correlate well with reflective patterns in the GPR profile.

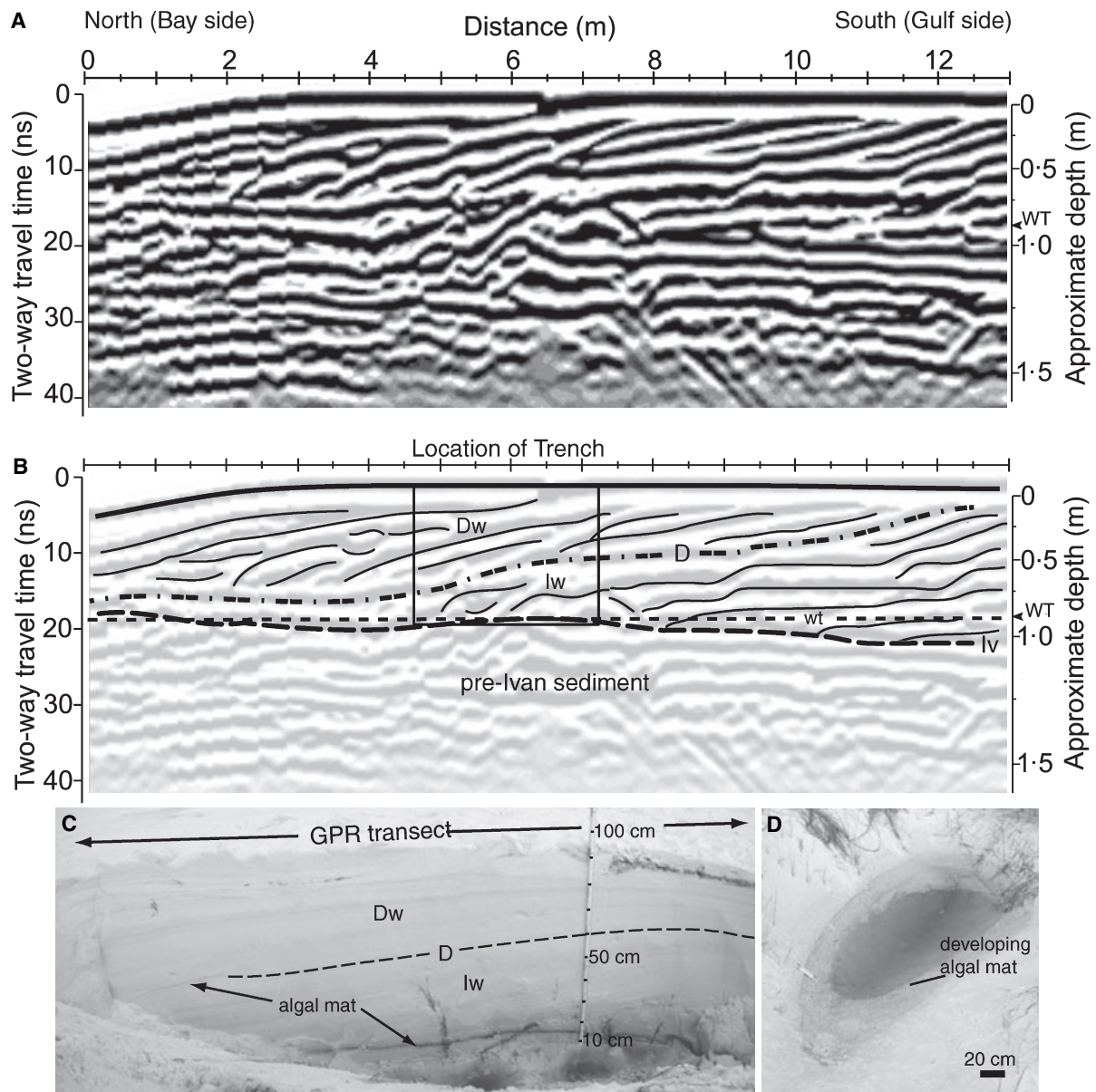


**Fig. 11.** (A) 250 MHz GPR transect scanned at the EG study site (Fig. 2D) following the passage of hurricane Dennis. The transect was scanned near the northern terminus of the Ivan-Dennis washover deposit, adjacent to the trench shown in the underlying photograph. The depth conversion is based on a velocity of  $0.12 \text{ m ns}^{-1}$  above the water table and  $0.06 \text{ m ns}^{-1}$  below. (B) Line-drawing interpretation of the profile showing: (1) radar surfaces D and Iv, interpreted to represent the base of the Dennis and Ivan washover deposits, respectively, (2) radar facies Dw (Dennis washover) and Iw (Ivan washover), and the position of the water table (wt). The Dw radar facies is characterized by dominantly north (landward) dipping downlapping reflections, while the Iv facies exhibits horizontal to sub-horizontal reflections merging landward into north-dipping downlapping reflections. Note that the water table lies coincident with radar surface Iv along much of the profile. The black box outline corresponds to the position of the trench shown in the photograph. (C) The trench excavated through the Dennis and Ivan washover deposits. The algal layer exposed in the base of the trench in conjunction with the buried marsh grasses mark the base of the Ivan washover deposit (Iw). A laterally discontinuous algal laminae is exposed on the north (left) side of the trench, separating the Dennis and Ivan washover units. A subtle angular discontinuity (dashed line labelled D) extends south from the algal laminae and represents the boundary between the Ivan and Dennis washover deposits. (D) Photograph of typical barrier island interior ephemeral pond showing laterally discontinuous algal mat development. Rapid burial by washover sediment results in preservation of the algal lamina.



**Fig. 12.** (A) Washover deposits in the barrier-island interior mangrove swamp produced by hurricanes Frances and Jeanne at the BG study site (Fig. 2F). The photograph was taken in January 2005, 4 months following the passages of Frances and Jeanne. (B) Photograph showing the overlapping Frances and Jeanne washover. The dashed line indicates the contact between the Frances and overlying Jeanne washover deposits.

action is expected in the bay under hurricane conditions. However, based on the GPR profiles, the prograding steep sigmoid foreset bedding and the tangential basal contact seem to indicate that the overwash transport and deposition into the back-barrier bay are still dominated by bedload, and that the sediment mixing by waves in the back bay is not significant.

## DISCUSSION

In the following, the erosional and depositional characteristics of the hurricane-induced regional-scale overwash in different sub-environments in a barrier island are summarized and compared. The studied barrier-island sub-environments include: (i) dune field, (ii) interior marsh, (iii) interior mangrove swamp, and (iv) back-barrier bay. Washover deposits also are controlled significantly by regional morphological and sedimentological conditions. This regional control is discussed based on the comparison of the Pan-

handle and southern Florida Atlantic coast washover.

Extensive overwash into the dune field is characterized by a sharp and horizontal basal erosional surface truncating the previous dune deposits. Depending on the age of the dune, vegetation type and density, the erosional surface can be distinctive (Fig. 6) or subtle (Fig. 7). Erosion of the dunes is driven mostly by wave action, as suggested by the extensive horizontal erosional surface. This dune erosion is a major supply of washover sediment to all the sub-environments. The dune erosion is also crucial in creating accommodation space for the deposition of subsequent washover deposits. The overwash platform replacing the eroded dune field is characterized by horizontal to slightly landward-dipping stratification.

Overwash into the interior marsh wetland is largely a depositional event, in contrast to the erosion and replacement of the dune field by a washover platform farther seaward. Little to no erosion occurred before the rapid deposition of



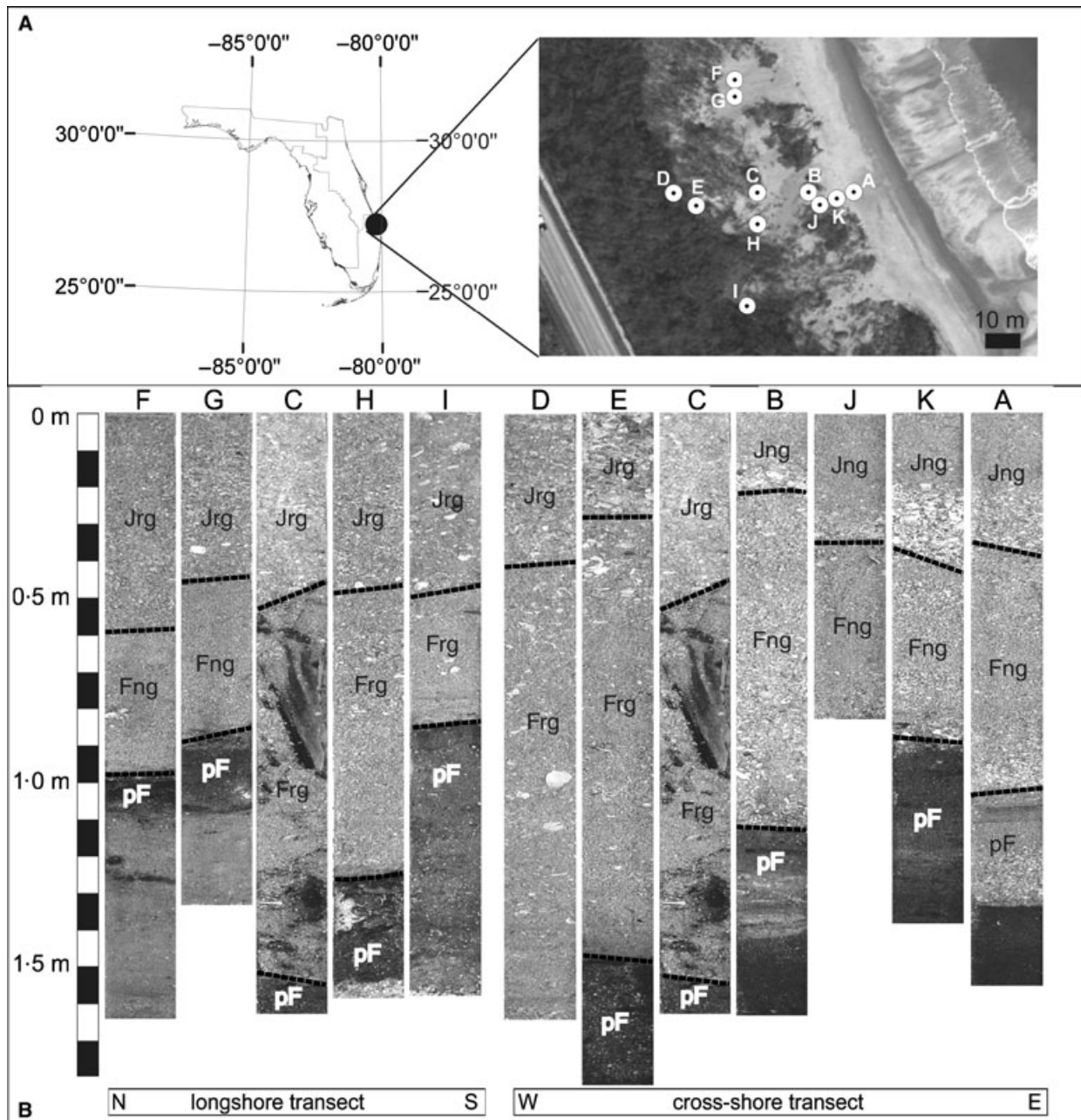


**Fig. 13.** Cores through the Frances and Jeanne washover deposits, collected at the BG study site. (A) Location map and aerial image of the BG site showing the core locations. The photograph was taken in September 2004 following the passage of hurricane Jeanne (photograph courtesy of NOAA), and shows the dense mangrove vegetation which dominates much of the interior portions of Hutchinson island. (B) Core photographs arranged in longshore (north-south) and cross-shore (west-east) transects. The washover deposits are underlain by peat, organic sand and limonite-stained sand layers (**pF** unit). The cross-shore transect shows both normally graded washover deposits (Frances – **Fng**; Jeanne – **Jng**) east of and including core B, and reverse graded bedding (Frances – **Frg**; Jeanne – **Jrg**) west of core B. The longshore transect illustrates dominantly reverse-graded bedding within both the Frances and Jeanne washover units.

the washover sediments, as indicated by the buried, sometimes upright, marsh grass (Fig. 8) and the preserved thin algal mat layer (Fig. 10). The contact between the washover deposits and the underlying organic-rich marsh sediments is

distinctive, although this sharp contact does not represent an erosional event. The thickness of washover sediment, typically greater than that over the eroded dune field, is controlled by the elevation of the marsh wetland.

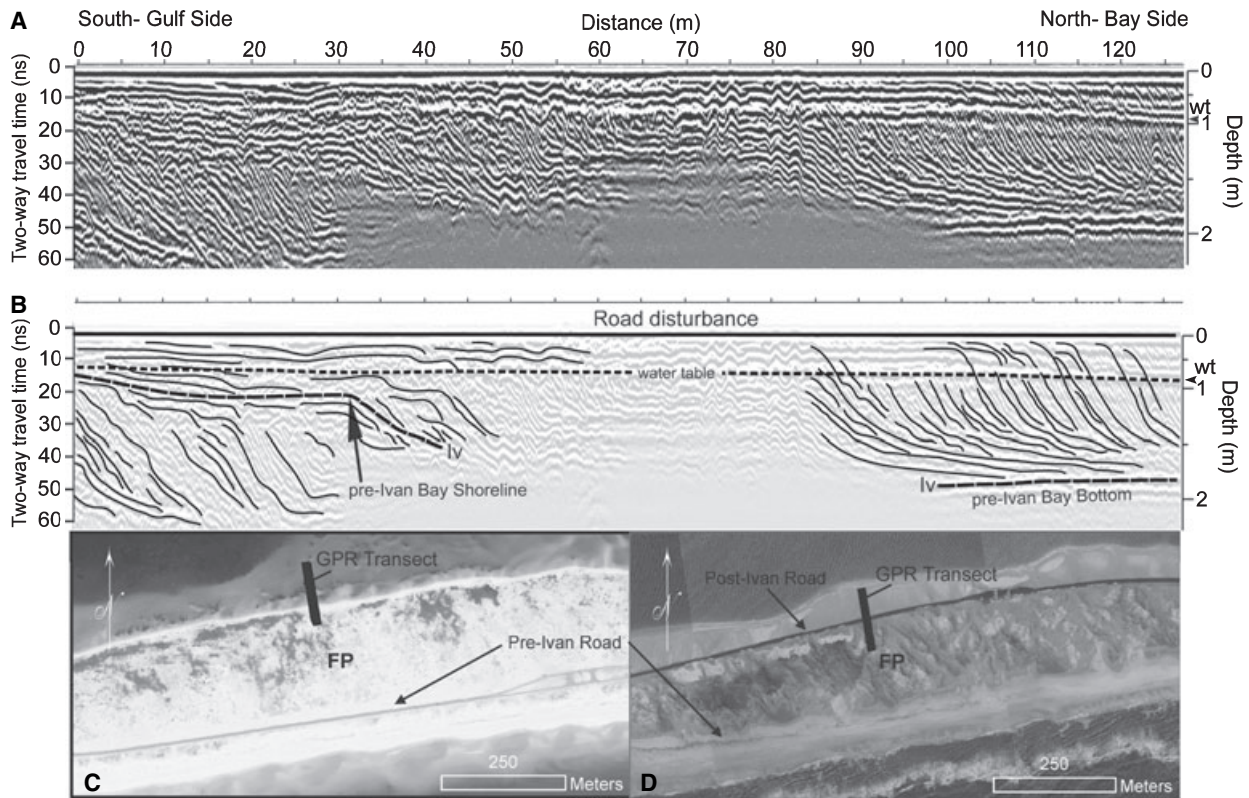


**Fig. 14.** (A) 250 MHz GPR transect scanned at the FP study site (Fig. 2A) post-Ivan and pre-Dennis. The depth conversion is based on a velocity of  $0.12 \text{ m ns}^{-1}$  above the water table and  $0.06 \text{ m ns}^{-1}$  below. (B) Line-drawing interpretation of the profile showing radar surface Iv, interpreted to represent the base of the Ivan washover deposit, and the position of the water table (wt). The radar facies representing the Ivan washover (above Iv) is characterized by sigmoidal, tangential and downlapping reflections. Similar reflective patterns are evident below Iv on the southern (Gulf-ward) portion of the profile, and probably represent an earlier washover deposit. The downwarping of Iv at 30 m correlates with the position of the pre-Ivan back-bay shoreline. (C and D) Pre- and post-Ivan aerial photographs of the study site. Photograph C was taken in March, 2004 (pre-Ivan) and shows the location of the GPR transect, the pre-Ivan shorelines, and a road which was subsequently destroyed during the passage of Ivan (photograph courtesy of Florida Department of Environmental Protection). Photograph D was taken in July 2005 following the passage of hurricane Dennis, and shows the location of the GPR transect, and the pre-Ivan and post-Ivan road positions (photograph courtesy of NOAA).

Overwash into the back-barrier bay yields the thickest washover deposits (up to 2 m thick) which is attributed to increased accommodation space. Based on the prograding sigmoid bedding and the tangential basal contact (Fig. 13), no significant erosional event appears to have preceded the washover deposition. Washover deposition occurred in a progradational manner dominated by bedload transport. It is therefore possible to distinguish the different barrier-island sub-environments before the regional overwash event based on the above distinctive washover characteristics.

Overwash along the southern Florida Atlantic coast is substantially different from the Panhandle overwash, controlled by the different morphological and sedimentological characteristics. The studied beach is backed by dense

mangrove with few or no dunes (Fig. 2F). The absence of dunes had significant influence on the penetration of the overwash bore and the deposition of washover sediments. The horizontal and steeply inclined bedding commonly observed in the Panhandle was not identified along the Florida Atlantic coast. In contrast, graded bedding, both normal and reversed, characterizes washover deposition within the mangrove swamp. The two overwash events (Frances and Jeanne) can be easily distinguished in plan view (Fig. 12), as well as in cores (Fig. 13). The formation of the graded bedding is probably caused by the intense interaction between the dense mangrove and the overwashing waves and currents, leading to selective sediment suspension and settling. This process contrasts the bedload-dominated transport and deposition in the other

studied sub-environments. The large range of sediment grain size provides the material for the graded bedding. The reason for the formation of the normal and reversed graded bedding is not exactly clear. Spatial distribution pattern seems to indicate that the intense interaction between waves and currents and dense mangrove tends to form reversed grading, while lesser interaction seaward of the dense mangrove swamp leads to normal graded bedding. The contact between the washover deposits and the organic-rich mangrove swamp sediment is distinctive. However, this sharp boundary does not represent an erosional event.

The very different washover deposits caused by Frances–Jeanne and Ivan–Dennis are largely controlled by the following two factors. First, the overall barrier-island morphology and vegetation played crucial roles. The Gulf-facing Panhandle barrier islands are characterized by extensive dune fields that are susceptible to erosion by hurricane-induced waves. Mangrove swamps dominate the studied Atlantic-facing barrier with few or no dunes separating the beach and the swamp. The dense mangroves may dissipate the energy carried by the overwashing waves and currents rapidly without supplying a large amount of new sediment. Secondly, the sediments at the two locations are very different, with the Panhandle sediments being very homogeneous and the Hutchison Island sediments being poorly sorted and very shelly. The different sediment properties influence the formation and identification of sedimentary structures.

## CONCLUSIONS

Regional-scale overwash occurred along the northern Florida barrier islands caused by hurricanes Ivan in 2004 and Dennis in 2005. Regional overwash, although to a lesser extent, also occurred along the southern Florida barrier islands, caused by hurricanes Frances and Jeanne. The washover deposits in the two regions are different in terms of regional extent, basal erosional features and sedimentary structures. Overall, the Ivan–Dennis washover deposits are characterized by horizontal and prograding steep foreset bedding, in contrast to graded bedding in the Frances–Jeanne washover. The different erosional and depositional characteristics are caused by the different overall barrier-island morphologies, vegetation types and densities, and sediment properties.

Different erosional and depositional characteristics were observed at different barrier-island sub-environments. Over the eroded dune fields, the base of the washover deposits is characterized by an extensive horizontal erosional surface, truncating the older dune deposits. Wave action is responsible for this erosional surface. The washover deposits demonstrate horizontal to slightly landward-dipping stratification. Washover deposits in the interior marsh wetlands are characterized by steep tabular bedding, with no erosional feature along the base. The thickest washover deposits of nearly 2 m were measured in the back-barrier bay, and are characterized by steeply inclined sigmoid bedding, prograding landward into the bay. Accommodation space controls the thickness of washover deposits in the different sub-environments. These different washover characteristics can be used to identify barrier-island sub-environments before the overwash event and, therefore, provide valuable insight into barrier-island evolution.

It is difficult to separate washover deposits from Ivan (2004) and Dennis (2005) along the Florida Panhandle coast, except locally, largely because of the homogeneity of the sediment grain size. Along the SE Florida barrier islands, overwash associated with hurricanes Frances and Jeanne penetrated into the dense interior mangrove swamps. There, washover deposits demonstrate two phases of graded bedding, both normal and reverse, and are probably the product of intense interaction between the overwashing wave current and the dense mangrove vegetation.

## ACKNOWLEDGEMENTS

The present study is supported by the University of South Florida and the Geography and Regional Science Program of the the National Science Foundation. We greatly appreciate the critical reviews of Dr Richard A. Davis, Jr and an anonymous reviewer.

## REFERENCES

- Andrews, P.B.** (1970) Facies and genesis of a hurricane washover fan, St. Joseph Island, Central Texas Coast. Report of Investigation No. 67, Bureau of Economic Geology, University of Texas at Austin, Austin, TX.
- Armbruster, C.K.** (1997) Morphologic Responses of a Low-Energy, Micro-Tidal Beach to Winter Cold Front Passages: North Shore Santa Rosa Island, Florida. MS thesis, Department of Geography and Anthropology,

- Louisiana State University, Baton Rouge, LA, 70803, 166 pp.
- Botha, G.A., Bristow, C.S., Naomi, P., Duller, G., Armitage, S.J., Roberts, H.M., Clarke, B.M., Kota, M.W. and Schoeman, P.** (2003) Evidence for dune reactivation from GPR profiles on the Maputaland coastal plain, South Africa. In: *Ground-penetrating Radar in Sediments* (Eds C.S. Bristow and H.M. Jol), *Geol. Soc. Lond. Spec. Publ.*, **211**, 29–46.
- Bristow, C., Pugh, J. and Goodall, T.** (1996) Internal structure of Aeolian dunes in Abu Dhabi determined using ground-penetrating radar. *Sedimentology*, **43**, 995–1003.
- 4 Buynevich, I.V., Fitzgerald, D.M. and Van Heteren, ?** (2004) Sedimentary records of intense storms in Holocene barrier sequences, Maine, USA. *Mar. Geol.*, **210**, 135–148.
- Clemmensen, L.B., Pye, K., Murray, A. and Heinemeier, J.** (2001) Sedimentology, stratigraphy and landscape evolution of a Holocene coastal dune system, Lodbjerg, NW Jutland, Denmark. *Sedimentology*, **48**, 3–27.
- Daniels, D.J., Gunton, D.J. and Scott, H.F.** (1988). Introduction to subsurface radar. *IEE Proc.*, **135**, 278–320.
- Davis, J.L. and Annan, A.P.** (1989) Ground-penetrating radar for high-resolution mapping of soil and rock stratigraphy. *Geophys. Prospect.*, **37**, 531–551.
- Davis, R.A., Jr and Barnard, P.L.** (2000) *How Anthropogenic Factors in the Back-barrier Area Influence Tidal Inlet Stability: Examples from the Gulf Coast of Florida, USA, Coastal and Estuarine Environments: Sedimentology, Geomorphology, and Geoarchaeology*. *Geol. Soc. Lond. Spec. Publ.*, **175**, 293–303.
- Dingler, J.R. and Reiss, T.E.** (1995) Beach erosion on Trinity Island, Louisiana caused by Hurricane Andrew. *J. Coast. Res.* (Special Issue), **21**, 254–264.
- Donnelly, C., Kraus, N.C. and Larson, M.** (2006) State of knowledge on measurements and modeling of coastal overwash. *J. Coast. Res.*, **22**, 965–992.
- Dougherty, A.J., Fitzgerald, D.M. and Buynevich, I.V.** (2004) Evidence for storm-dominated early progradation of Castle Neck barrier, Massachusetts, USA. *Mar. Geol.*, **210**, 123–134.
- Fisher, J.S., Leatherman, S.P. and Perry, F.C.** (1974) *Overwash Processes on Assateague Island*. Proceedings of 14th International Conference on Coastal Engineering, ASCE press, ????, pp. 1194–1212.
- Hayes, M.O.** (1967) Hurricanes as geological agents, south Texas coast. *Am. Assoc. Petrol. Geol. Bull.*, **51**, 937–942.
- Horwitz, M.H. and Wang, P.** (2005) Sedimentological characteristics and internal architecture of two overwash fans from Hurricanes Ivan and Jeanne. *GCAGS Trans.*, **55**, 342–352.
- Jol, H.M., Smith, D.G. and Meyers, R.A.** (1996) Digital ground-penetrating radar (GPR): an improved and very effective geophysical tool for studying modern coastal barriers (examples from the Atlantic, Gulf and Pacific coasts, U.S.A.). *J. Coast. Res.*, **12**, 960–968.
- Leatherman, S.P.** (1977) *Overwash Hydraulics and Sediment Transport*. Proceedings of Coastal Sediments '77, ASCE
- 5 Press, ????, pp. 135–148.**
- Leatherman, S.P.** (1987) Coastal geomorphological applications of ground-penetrating radar. *J. Coast. Res.*, **3**, 397–399.
- Leatherman, S.P. and Williams, A.T.** (1977) Lateral textural grading in overwash sediments. *Earth Surf. Proc. Land.*, **2**, 333–341.
- Leatherman, S.P. and Williams, A.T.** (1983) Vertical sedimentation units in a barrier island washover fan. *Earth Surf. Proc. Land.*, **8**, 141–150.
- Leatherman, S.P., Williams, A.T. and Fisher, J.S.** (1977) Overwash sedimentation associated with a large-scale northeaster. *Mar. Geol.*, **24**, 109–121.
- Møller, I. and Anthony, D.** (2003) GPR study of sedimentary structures within a transgressive coastal barrier along the Danish North Sea coast. In: *Ground-penetrating Radar in Sediments* (Eds C.S. Bristow and H.M. Jol). *Geol. Soc. Lond. Spec. Publ.*, **211**, 55–67.
- Morang, A.** (1992) Inlet migration and hydraulic processes at East Pass, Florida. *J. Coast. Res.*, **18**, 486–501.
- Morton, R.A.** (1978) Large-scale rhomboid bed forms and sedimentary structures associated with hurricane washover. *Sedimentology*, **25**, 183–204.
- Morton, R.A. and Sallenger, A.H. Jr.** (2003) Morphological impacts of extreme storms on sandy beaches and barriers. *J. Coast. Res.*, **19**, 560–574.
- Neal, A.** (2004) Ground-penetrating radar and its use in sedimentology: principles, problems and progress. *Earth-Sci. Rev.*, **66**, 261–330.
- Nordstrom, K.F.** (1992) *Estuarine Beaches*. Elsevier Applied
- 6 Science, ?????, 225 pp.**
- Nordstrom, K.F. and Roman, C.T.** (Eds.) (1996) *Estuarine Shores: Evolution, Environments and Human Alterations*. Wiley, New York, 486 pp.
- Sallenger, A.H.** (2000) Storm impact scale for barrier islands. *J. Coast. Res.*, **16**, 890–895.
- Schwartz, R.K.** (1975) Nature and genesis of some storm washover deposits. CERC Technical Memo 61, U.S. Army Corps of Engineers, 69 p.
- Schwartz, R.K.** (1982) Bedform and stratification characteristics of some modern small-scale washover sand bodies. *Sedimentology*, **29**, 835–849.
- Sedgwick, P.E. and Davis, R.A. Jr.** (2003) Stratigraphy of washover deposits in Florida: implications for recognition in the stratigraphic record. *Mar. Geol.*, **200**, 31–48.
- Sheriff, R.E.** (1977) Limitations on resolution of seismic reflections and geologic detail derivable from them. In: *Seismic Stratigraphy—Applications to Hydrocarbon Exploration* (Ed. C.E. Payton), *AAPG Mem.*, **16**, 3–14.
- Stapor, F.W.** (1973) History and sand budgets of the barrier island system in the Panama City, Florida region. *Mar. Geol.*, **14**, 277–286.
- Stone, G.W. and Stapor, F.W.** (1996) A nearshore sediment transport model for the Northeast Gulf of Mexico Coast. *J. Coast. Res.*, **12**, 786–792.
- Stone, G.W., Liu, B., Pepper, D.A. and Wang, P.** (2004) The importance of extratropical and tropical cyclones on the short-term evolution of barrier islands along the northern Gulf of Mexico, USA. *Mar. Geol.*, **210**, 63–78.
- Stone, G.W., Walker, N.D., Hsu, S.A., Babin, A., Liu, B., Keim, D., Teague, W., Mitchell, D. and Leben, R.** (2005) Hurricane Ivan's impact along the Northern Gulf of Mexico. *EOS Trans. Am. Geophys. Union*, **86**, 497–508.
- Wang, D.W., Mitchell, D.A., Teague, W.J., Jarosz, E. and Hulbert, M.S.** (2005) Extreme waves under Hurricane Ivan. *Science*, **309**, 896.
- Wang, P., Kirby, J.H., Haber, J.D., Horwitz, M.H., Knorr, P.O. and Krock, J.R.** (2006) Morphological and sedimentological impacts of hurricane Ivan and immediate post-storm beach recovery along the northwestern Florida barrier-island coasts. *J. Coast. Res.*, **22**, in press.

Manuscript received 28 April 2006; revision accepted 23 October 2006

# Author Query Form

Journal: SED

Article: 848

Dear Author,

During the copy-editing of your paper, the following queries arose. Please respond to these by marking up your proofs with the necessary changes/additions. Please write your answers on the query sheet if there is insufficient space on the page proofs. Please write clearly and follow the conventions shown on the attached corrections sheet. If returning the proof by fax do not write too close to the paper's edge. Please remember that illegible mark-ups may delay publication.

Many thanks for your assistance.

Query reference	Query	Remarks
1	<b>Au: Please supply a short title of up to 40 characters.</b>	
2	<b>Au: Please check: 'used to ground truth'</b>	
3	<b>Au: Please define: WAAS.</b>	
4	<b>Au: Please provide initials of 'Van Heteren'</b>	
5	<b>Au: Please provide location (city) of 'ASCE Press'</b>	
6	<b>Au: Please provide location (city) of 'Elsevier Applied Science'</b>	

# MARKED PROOF

## Please correct and return this set

Please use the proof correction marks shown below for all alterations and corrections. If you wish to return your proof by fax you should ensure that all amendments are written clearly in dark ink and are made well within the page margins.

<i>Instruction to printer</i>	<i>Textual mark</i>	<i>Marginal mark</i>
Leave unchanged	... under matter to remain	Ⓟ
Insert in text the matter indicated in the margin	∧	New matter followed by ∧ or ∧ <sup>Ⓢ</sup>
Delete	/ through single character, rule or underline or ┌───┐ through all characters to be deleted	Ⓞ or Ⓞ <sup>Ⓢ</sup>
Substitute character or substitute part of one or more word(s)	/ through letter or ┌───┐ through characters	new character / or new characters /
Change to italics	— under matter to be changed	↙
Change to capitals	≡ under matter to be changed	≡
Change to small capitals	≡ under matter to be changed	≡
Change to bold type	~ under matter to be changed	~
Change to bold italic	≈ under matter to be changed	≈
Change to lower case	Encircle matter to be changed	≡
Change italic to upright type	(As above)	⊕
Change bold to non-bold type	(As above)	⊖
Insert 'superior' character	/ through character or ∧ where required	Υ or Υ under character e.g. Υ or Υ
Insert 'inferior' character	(As above)	∧ over character e.g. ∧
Insert full stop	(As above)	⊙
Insert comma	(As above)	,
Insert single quotation marks	(As above)	Ƴ or ƴ and/or ƶ or Ʒ
Insert double quotation marks	(As above)	ƶ or Ʒ and/or Ʒ or ƶ
Insert hyphen	(As above)	⊥
Start new paragraph	┌	┌
No new paragraph	┐	┐
Transpose	┌┐	┌┐
Close up	linking ○ characters	⸸
Insert or substitute space between characters or words	/ through character or ∧ where required	Υ
Reduce space between characters or words		↑